Pharm Res (2015) 32:2736–2752
DOI 10.1007/s11095-015-1659-5

RESEARCH PAPER

Synthesis and Evaluation of Substituted Poly(organophosphazenes) as a Novel Nanocarrier System for Combined Antimalarial Therapy of Primaquine and Dihydroartemisinin

Sahil Kumar • Rajesh K. Singh • R. S. R. Murthy • T. R. Bhardwaj

Received: 1 November 2014 / Accepted: 18 February 2015 / Published online: 17 March 2015

ABSTRACT

Purpose The synthesis and evaluation of novel biodegradable poly(organophosphazenes) (**3**–**6**) namely poly[bis-(2-propoxy)]phosphazene **(3)** poly[bis(4-acetamidophenoxy)]phosphazene **(4)**poly[bis(4-formylphenoxy)]phosphazene **(5)** poly[bis(4-ethoxycarbonylanilino)]phosphazene **(6)** bearing various hydrophilic and hydrophobic side groups for their application as nonocarrier system for antimalarial drug delivery is described.

Methods The characterization of polymers was carried out by IR, ^{1}H-NMR and ^{31}P-NMR. The molecular weights of these novel polyphosphazenes were determined using size exclusion chromatography with a Waters 515 HPLC Pump and a Waters 2414 refractive index detector. The degradation behavior was studied by 200 mg pellets of polymers in phosphate buffers pH 5.5, 6.8 and 7.4 at 37°C. The degradation process was monitored by changes of mass as function of time and surface morphology of polymer pellets. The developed combined drugs nanoparticles formulations were evaluated for antimalarial potential in *P. berghei* infected mice.

Results These polymers exhibited hydrolytic degradability, which can afford applications to a variety of drug delivery systems. On the basis of these results, the synthesized polymers were employed as nanocarriers for targeted drug delivery of primaquine and dihydroartemisinin. The promising *in vitro* release of both the drugs from nanoparticles formulations provided an alternative therapeutic combination therapy regimen for the treatment of drug resistant malaria. The nanoparticles formulations tested in resistant strain of *P. berghei* infected mice showed 100% antimalarial activity.

Conclusions The developed nanocarrier system provides an alternative combination regimen for the treatment of resistant malaria.

KEY WORDS biodegradable polyphosphazenes · degradation · dihydroartemisinin · drug-resistant malaria · nanoparticles · primaquine

ABBREVIATIONS

^{1}H-NMR	Proton nuclear magnetic resonance
^{31}P-NMR	Phosphorus nuclear magnetic resonance
ALP	Alkaline phosphatase
ANOVA	Analysis of variance
CPCSEA	Committee for the purpose of control and supervision on experiments on animals
D_2O	Deuterated water

Electronic supplementary material The online version of this article (doi:10.1007/s11095-015-1659-5) contains supplementary material, which is available to authorized users.

S. Kumar • R. S. R. Murthy • T. R. Bhardwaj (✉)
Polymer Chemistry and Technology Research Laboratory, Department of Pharmaceutical Chemistry, Indo-Soviet Friendship (I.S.F) College of Pharmacy, Ferozepur Road, Moga 142001, Punjab, India
e-mail: bhardwajrtilak@yahoo.com

S. Kumar
e-mail: sahil.mehta187@gmail.com

R. K. Singh
Department of Pharmaceutical Chemistry, Shivalik College of Pharmacy, NangalDist. Ropar, 140126, Punjab, India

T. R. Bhardwaj
University Institute of Pharmaceutical Sciences, Panjab University, Chandigarh 160014, India

S. Kumar
Research Scholar, Punjab Technical University, Jalandhar, Jalandhar-Kapurthala Highway, Kapurthala 144601, India

DHA	Dihydroartemisinin
DMSO	Dimethyl sulphoxide
DSC	Differential scanning calorimetry
EDTA	Ethylene diamine tetraacetic acid
EE	Entrapment efficiency
ELISA	Enzyme linked immuno sorbent assay
HPLC	High performance liquid chromatography
IAEC	Institutional animal ethical committee
IR	Infrared
MHz	Mega hertz
MST	Mean survival time
M_w	Molecular weight
NIMR	National institute of malaria research, New Delhi, India
NP	Nanoparticles
o/w	Oil/water
PBS	Phosphate buffer saline
PEG	Polyethyleneglycol
ppm	parts per million
PQ	Primaquine
RBCs	Red blood cells
SEM	Scanning electron microscopy
SGOT	Serum glutamic oxaloacetic transaminase
SGPT	Serum glutamic pyruvate transaminase
TEM	Transmission electron microscopy
T_g	Glass transition temperature
TGA	Thermogravimetric analysis
THF	Tetrahydrofuran
UV	Ultraviolet
Wt	Weight

INTRODUCTION

Polyphosphazenes are polymers having an inorganic backbone and composed of nitrogen and phosphorus atoms linked by alternating single and double bonds with two substituent at each phosphorus atom. These are the most versatile inorganic polymers because a wide variety of substituents can be attached to the backbone phosphorus atom which result in a very broad spectrum of physical as well as chemical properties suitable for many potential applications, including biomedical applications and polymeric drug delivery systems (1,2). The major precursor, polydichlorophosphazene, is extremely hydrolytically unstable but can be readily substituted with nucleophilic substituents to give a wide range of stable poly(organophosphazenes) with an extremely wide range of properties (Fig. 1) (3).

The synthetic flexibility and versatile adaptability has resulted in an enormous number of materials with a wide range of biomedical applications (4), varying from water soluble polyphosphazenes (5) to superhydrophobic polymers (Fig. 2) (6).

Depending on the side groups applied, polyphosphazenes can be biodegradable, which opens up routes for applications in the area of tissue engineering and drug delivery (7–9). Polyphosphazenes can undergo hydrolytic degradation by both surface and bulk erosion (10). Recently, poly(organophosphazenes) having hydrophilic PEG chains conjugated with hydrophobic isoleucine ethyl ester groups have also been prepared for the sustained delivery of the anticancer drugs 5-fluorouracil (11) and doxorubicin. The glycyl lactate ethyl esters sensitive to hydrolysis were also added to enhance polymer degradation (12). The various substituted polyphosphazenes have been employed as targeted drug delivery systems by our research group (13,14). Further, one of our co-author has valuable contribution to the development of implants for antimalarial drug chloroquine using biodegradable polymers such as gelatin and cross-linked gelatin. The implants were evaluated for physicochemical properties, *in vitro* drug release study and pharmacokinetics. The results revealed that the implants exhibited optimum drug release which conform to the prerequisite of a long term implant for 7 days (15). There was another contribution to the artemether (**8**) loaded lipid nanoparticles formulations developed by modified thin-film hydration method which were found to be safe and more potential as antimalarial when compared with standard and marketed formulations (16).

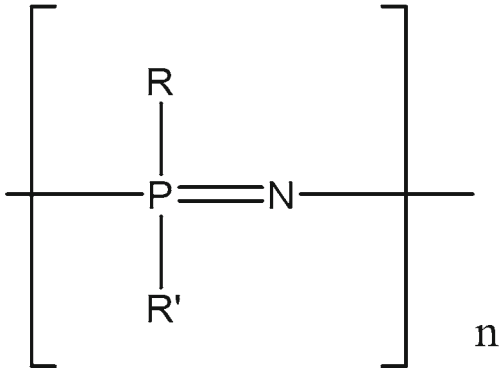

Fig. 1 General structure of poly(organophosphazenes).

In connection with the relevant research work envisaged for the design, synthesis and evaluation of nanoparticles of polymer linked combined antimalarial drugs for the treatment of drug-resistant malaria, contributed by our research group (17), we attempted to synthesize and evaluate some controlled molecular weight substituted poly(organophosphazenes) bearing various hydrophilic and hydrophobic side groups so as to develop these polymers to be used as nanocarriers for the targeted and sustained delivery of antimalarial drugs. Although various polymers have been employed for the targeted drug delivery of primaquine and other antimalrial drugs but the substituted polyphosphazenes have not been employed as novel carrier materials for the drug delivery applications. The synthesized substituted poly(organophosphazenes) were employed as nanocarriers materials for combined regimen of primaquine (PQ) and dihydroartemisinin (DHA) antimalarials for the treatment of drug resistant strains of malaria. The objective of the present study was to develop a novel and effective drug delivery

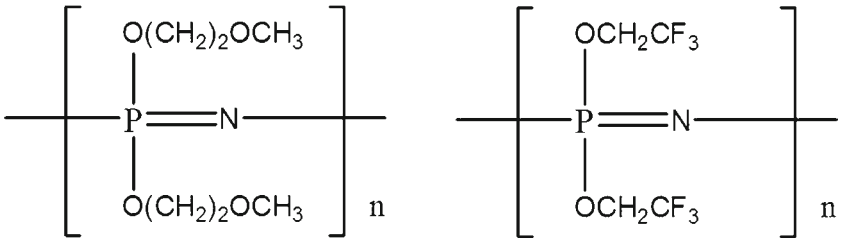

Fig. 2 Some examples of poly(organophosphazenes) with varied properties.

system for increasing the uptake of both antimalarial drugs by malarial parasite infected cells. This could be accomplished only after the formulation of nanoparticles. Further, the combination regimen is effective to treat the drug-resistant malaria as both the drugs (primaquine and dihydroartemisinin) have different mechanisms of action.

EXPERIMENTAL METHODS

Materials

Trimer was obtained from Sigma-Eldrich and was purified by petroleum ether before synthesis of poly(dichlorophosphazene). Tetrahydrofuran was dried by refluxing with sodium using benzophenone and kept over sodium wire. The ^{1}H-NMR and ^{31}P-NMR spectra were recorded on Brucker Avance II 400 MHz NMR spectrometer. The molecular weights of polyphosphazenes were determined using size exclusion chromatography with a Waters 515 HPLC Pump and a Waters 2414 refractive index detector. THF was used as solvent with a flow rate of 1 ml/min at 40°C and narrow disperse polystyrene as calibration standards. Thermogravimetric analysis (TGA) measurements were carried out by a TGA, TA SDT Q60 (at a heating rate of 10°Cmin^{-1}). Differential scanning calorimetric (DSC) measurements were carried out with a DSC, Q20, TA- Instruments Waters (LLC, USA). The calorimeter was calibrated for temperature and heat flow accuracy using the melting of pure indium (mp 156.6°C and δH of 25.45 Jgm^{-1}). 3–5 mg of samples were loaded in sealed non-hermetic aluminium pans and were run within temperature range of 50–400°C with a heating rate of 10°C per minute under nitrogen atmosphere (flow rate 50 cc/min). The data were managed by TA Q series Advantage software (Universal analysis 2000).

The morphology of the drug loaded substituted polyphosphazenes nanoparticles was analyzed by the transmission electron microscopy (TEM) by using the stain phosphotungstic acid. A drop of nanoparticle formulation was spread on a 200-mesh, copper grid coating and the droplets excess were removed onto the filter paper. After 5 min, a drop of 2% phosphotungstic acid was placed onto the copper grid. The grid was dried at room temperature and observed by TEM.

The average particle size, size distribution and Zeta potential of the drug loaded nanoparticles was determined by using Delsa NanoC Zeta sizer (Beckman. Coulter Pvt. Ltd.). The nanoparticles formulation was put into the polystyrene latex cell and measured at the detector angle of 90°C having a wavelength of 633 nm, a refractive index (1.59), and a temperature of 25°C was maintained.

METHODS

Preparation and Characterization of Polymers

The synthesis of various substituted poly(organophosphazenes) was carried out according to Scheme I.

Synthesis of Poly(dichlorophosphazene) (2)

The trimer material hexachlorocyclotriphosphazene **(1)** was polymerized to poly(dichlorophosphazene) **(2)** by the procedure reported in literature (18).

Synthesis of Poly[bis-(2-propoxy)]phosphazene (3)

Sodium metal (4.60 g, 0.2 mol) was added in small portions to 2-propanol (12.0 g, 0.2 mol) taken in a two necked round bottom flask fitted with a reflux condenser. The reaction mixture was refluxed in an oil bath till all the metal had reacted. After completion of the reaction, the excess of 2-propanol was distilled off under reduced pressure to get sodium 2-propoxide. A solution of sodium 2-propoxide (15.0 g, 0.183 mol) in dry tetrahydrofuran (THF) (150 ml) was added dropwise to the solution of poly(dichlorophosphazene) (10.0 g, 0.087 mol) (**2**), in THF and refluxed for 3 days under inert atmosphere, cooled, filtered and concentrated under reduced pressure. The product was precipitated with water to get pure poly[bis-(2-propoxy)]phosphazene **(3)**. In order to remove unreacted molecules and inorganic salt, the solution was dialyzed for 2 days against distilled water using cellulose dialysis membranes (molecular weight cutoff: 3.5×10^3). The dialyzed solution was freeze dried to obtain polymer **(3).**

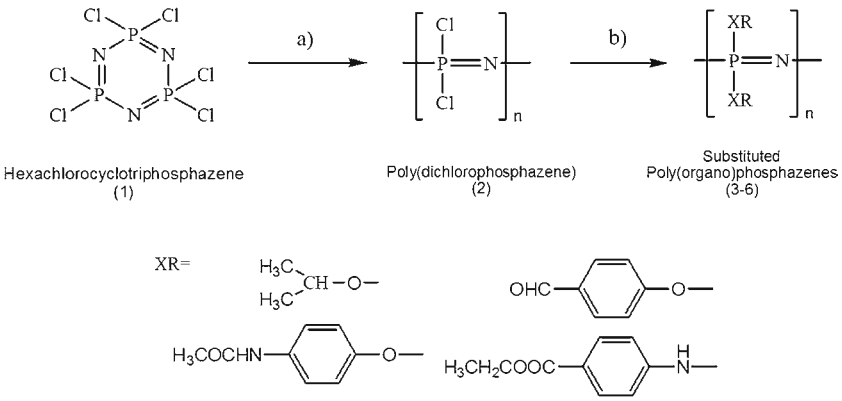

Scheme I General Scheme for the synthesis of substituted poly(organophosphazenes): (**a**) Δ, 240 ± 5°C, anhydrous $AlCl_3$, (**b**) Sodium isopropoxide/potassium 4-acetomidophenoxide/potassium 4-formylphenoxide/4-aminobenzoic acid, THF, reflux.

Synthesis of Poly[bis(4-acetamidophenoxy)] phosphazene (4)

4-Hydroxyacetanilide (30.0 g, 0.199 mol) was dissolved in dry ethyl methyl ketone (200 ml). To this solution was added potassium carbonate (60.0 g, 0.435 mol) in small portions. The reaction mixture was refluxed under inert atmosphere for 5 h., filtered, residue washed with ethyl methyl ketone and dried to get potassium 4-acetamidophenoxide. A solution of potassium 4-acetamidophenoxide (32.60 g, 0.172 mol) in dry tetrahydrofuran (200.0 ml) was added slowly with stirring to a solution of poly(dichlorophosphazene) (**2**) (10.0 g, 0.087 mol) in dry tetrahydrofuran (200.0 ml) under nitrogen atmosphere. The reaction mixture was refluxed for 80 h, filtered, and solvent removed under reduced pressure to get the concentrate. After the filtrate was evaporated, the concentrate which was taken in tetrahydrofuran precipitated using a solvent pair of ethanol and (1:2*v*/*v*) to obtain precipitate, which was repeated twice in the same solvent systemto get poly[bis(4-acetamidophenoxy)]phosphazene **(4).** In order to remove unreacted molecules and inorganic salt, the solution was dialyzed for 2 days against distilled water using cellulose dialysis membranes (molecular weight cutoff: 3.5×10^3). The dialyzed solution was freeze dried to obtain polymer (**5**).

Synthesis of Poly[bis(4-formylphenoxy)]phosphazene (5)

Potassium carbonate (50.0 g, 0.362 mol) was added in small portions to the solution of 4-hydroxybenzaldehye (25.0 g, 0.205 mol) in ethyl methyl ketone (200.0 ml) under inert atmosphere and refluxed for 5 h. After completion of the reaction the precipitated material was filtered, washed with ethyl methyl ketone and dried to obtain potassium 4-formylphenoxide. Poly(dichlorophosphazene) (**2**) (10.0 g, 0.087 mol) in dry tetrahydrofuran (200.0 ml) was added dropwise to the slurry of potassium 4-formylphenoxide (27.60 g, 0.173 mol) in tetrahydrofuran (200.0 ml). The reaction mixture was refluxed for 72 h, filtered, and concentrated to get poly[bis(4-formylphenoxy)] phosphazene. The polymer so obtained was purified by using solvent system water, ethanol and n-heptane (2:1:1 *v*/*v*). In order to remove unreacted molecules and inorganic salt, the solution was dialyzed for 2 days against distilled water using cellulose dialysis membranes (molecular weight cutoff: 3.5×10^3). The dialyzed solution was freeze dried to obtain polymer (**5**).

Synthesis of Poly[bis(4-ethoxycarbonylanilino)] phosphazene (6)

4-Aminobenzoic acid (0.291 mol) was added to absolute ethyl alcohol (250.0 ml) previously saturated with hydrochloric acid gas. The reaction mixture was refluxed for 2 h, poured into water and neutralized with sodium carbonate. Precipitated material was filtered, dried and crystallized from methanol to get ethyl 4-aminobenzoate. Freshly polymerized poly(dichlorophosphazene) (2) (10.0 g, 0.087 mol) was dissolved in dry toluene (200.0 ml). Freshly distilled triethylamine (10.0 ml) was added into the polymer solution followed by dropwise solution of ethyl 4-aminobenzoate (28.44 g, 0.172 mol) in dry THF (200.0 ml). The reaction mixture was refluxed for 170 h, cooled to room temperature and filtered to remove hydrochloride salts. The clear filtrate was concentrated under vacuum and precipitation by petroleum ether (60–80°C) to get the product. In order to remove unreacted molecules and inorganic salt, the solution was dialyzed for 2 days against distilled water using cellulose dialysis membranes (molecular weight cutoff: 3.5×10^3). The dialyzed solution was freeze dried to obtain polymer **(6)**.

In Vitro Degradation Studies

The *in vitro* degradation studies of poly(organophosphazene) were carried out by measuring weight loss as a function of time (days). For this experiment preweighed polymer pellets of 200 mg were placed in 50 ml of phosphate buffer solutions of pH 5.5, 6.8 and 7.4 at 37°C in a shaking incubator. Samples were withdrawn at time interval of 7, 14, 21, 28 and 35 days, dried in vacuum desiccator and then weighed to determine the weight loss. The

experiment was performed in triplicate. The results were expressed as percent mass loss *versus* time (19).

Scanning Electron Microscopy (SEM)

The morphologies of degraded samples of poly(organophosphazenes) were examined by scanning electron microscope (JEOL, JSM 6490, Japan) and (JSM 6100, Japan). Since moisturized materials cannot be detected by SEM, samples were dried in vacuum desiccator. Prior to imaging, the samples were fixed and dehydrated. Samples were subjected to SEM at voltages ranging from 10 to 25 kV after the samples were sputter-coated in white gold.

Thermal Properties

Thermal stability is one of the most important properties of poly(organophosphazenes). The decomposition temperatures and glass transition temperatures (T_g) were measured by thermogravimetry and differential scanning calorimetry, respectively.

Preparation of Nanoparticles (NP) Formulations

The different drug loaded nanoparticles formulations were formulated by a simple o/w emulsion diffusion method. Briefly, specific polymer and both the drugs were dissolved in dichloromethane and 50 ml of this organic solution was poured on 100 ml of aqueous solution containing 1% Tween 80 as a surfactant. This biphasic system was emulsified using mechanical stirrer at a speed of 3000 rpm for 2 h followed by homogenization at 7000 rpm during 10 min. The above dichloromethane solution was sonicated using probesonicator for 5 min. Finally, the organic solvent was evaporated under vacuum at 35°C, which results in stable nanoparticles formulations.

Physicochemical Characterization of Nanoparticles (NP) Formulations

Morphology, Particle Size and Zeta Potential Analysis

The morphology of the drug loaded substituted poly(organophosphazenes) nanoparticles was analyzed by the transmittance electron microscopy by using the stain phosphotungstic acid. A drop of nanoparticle formulation was spread on a 200-mesh, copper grid coating and the droplets excess were removed onto the filter paper. After 5 min, a drop of 2% phosphotungstic acid was placed onto the copper grid. The grid was dried at room temperature and observed by TEM.

The average particle size, size distribution and Zeta potential of the nanoparticles was determined by using Delsa NanoC Zeta sizer (Beckman. Coulter Pvt. Ltd.). The nanoparticles formulation was put into the polystyrene latex cell and measured at the detector angle of 90°C having a wavelength of 633 nm, a refractive index (1.59), and a temperature of 25°C was maintained.

Percentage Yield

The nanoparticles from each formulation were weighed and the respective percentage yield was calculated using the following formula (20).

$$\text{Percentage yield} = \text{wt of nanoparticles obtained/wt of drug and polymer used} \times 100$$

Percentage Entrapment Efficiency

To determine primaquine and dihydroartemisinin entrapment in nanoparticles formulations, the samples were analyzed by HPLC and % entrapment efficiency (EE) was calculated using following equation

$$\%\ \text{Yield} = 1 - \text{Free drug/theoretical drug loaded} \times 100$$

Drug Loading

The percentage drug loading was calculated by using following equation

$$\text{Percentage drug loading} = \text{Wt of drug in nanoparticles/Wt of nanoparticles taken} \times 100$$

In Vitro Drug Release Studies

The *in vitro* release studies was carried out by dialysis bag method pooling out known amount of nanoparticles in an activated dialysis bag (Molecular weight cutoff: 14,000; Sigma Aldrich), the bag was placed in methanolic phosphate buffer saline at pH 7.4. The release medium was maintained at stirring speed of 100 rpm and 37°C in shaking incubator. The sampling of 1 ml was done from the receptor section at regular time intervals up to 96 h and replaced with an equal volume of fresh PBS buffer. The concentration of free drug from the receptor was analyzed for primaquine by UV at 259 nm

and dihydroartemisinin by HPLC at λ_{max} 210 nm using Acetonitrile: Water (60:40) respectively. All the measurements were performed in triplicate. The linearity of primaquine was plotted in concentration range of 4 μg/ml to 12 μg/ml at λ_{max} 259 while that of dihydroartemisinin linearity was plotted in range of 100 μg/ml to 500 μg/ml at λ_{max} 210.

The data was analysed by fitting to the different kinetic models such as zero order, first order, Higuchi, Korsmeyer and Peppas. The release data obtained were treated according to zero-order (cumulative amount of drug release *versus* time), first-order (log cumulative percentage of drug remaining *versus* time), Higuchi (cumulative percentage of release *versus* square root of time) and Korsmeyer-Peppas (log cumulative percentage of drug released *versus* log time) equation models. The mechanism of release kinetics can be determined from correlation coefficient. The correlation coefficient getting close to 1.0 for a particular formulation, that release kinetics mechanism will be followed for that proposed formulation. The graphical method was used to determine the correlation coefficients.

Evaluation of Antimalarial Efficacy in P. berghei Infected Mice

The biological evaluation of designed nanoparticles formulations for antimalarial potential was carried out after getting approval from Institutional Animal Ethics Committee (IAEC) of the I.S.F. College of Pharmacy, Moga (Punjab) under protocol no.145. All the experiments on animals were performed as per the guidelines of Committee for the Purpose of Control and Supervision on Experiments on Animals (CPCSEA). The swiss albino mice weighing between 25–30 g and four to five weeks old were procured and fed with standard pellet diet and water *ad libitum*.

The *Plasmodium berghei* (NK 65) resistant strain was used as the source of parasites and procured from the National Institute Malaria Research (NIMR), New Delhi. All the animals were infected with 10^6 *P. berghei* by intraperitonial (i/p) route. After the development of infection, the animals were kept under observation to record mean percent parasitaemia, mean survival time and survival rate after giving treatment with drug loaded nanoparticles formulations to evaluate therir antimalarial efficacy.

The animals were divided according to the approved animal protocol as per the guidelines of CPCSEA. The parasitemia progression was monitored by observing under microscope (100 ×) after examining the thin smears of blood from the tail vein of mice. The parasitemia level was counted per 1000 RBC's per slide after taking 2–3 drops of blood from tail vein of mice, put on slide, air dried, fixed with methanol and stained with Giemsa. The average parasitemia was measured by counting a minimum of five fields (200 Red Blood Cells (RBCs) for each field) in one slide. The percent parasitemia was ccomputed using the following formula (21).

$$\text{Percent Parasitemia} = \text{No. of parasite RBCs/Total no. of RBCs examined} \times 100$$

Statistical Analysis

The graph pad prism was used to analyze data obtained and these were expressed as mean ± standard error of mean. The differences between means were compared using One way analysis of variance (ANOVA) followed by Dunnet's post hoc test. $P \leq 0.05$ were considered significant.

Determination of Average Percent Antimalarial Activity

The average percent antimalarial activity (= percent suppression) was determined according to the following formula

$$\text{Activity} = 1 - \text{Mean parasitemia of treated group/Mean parasitemia of control group}$$

Determination of Mean Survival Time

Mortality was monitored daily and the number of days from the time of incoculation of the parasite up to death was recorded for each mouse in the treatment and control groups throughout the follow up period. The mean survival time was determined for mice during an observation period of 35 days. The mean survival time (MST) for each group was calculated by the following formula (22).

$$\text{MST} = \text{Sum of survival time of all mice in a group (days)/ Total number of mice in that group}$$

In Vitro Erthrocytic Toxicity Assay

To run the erythrocytic toxicity test, the anticoagulant EDTA was added to 5 ml of whole blood samples from a healthy volunteer. Blood was centrifuged at 3000 rpm for 20 min in centrifuge. Buffy coat was removed and the packed cells were washed thrice with normal saline solution.

Briefly, to prepare the negative control, a volume of 100 µl cell suspension was added to 3 ml normal saline solution. The sample showed no haemolysis, i.e. red blood cells (RBCs) have not lysed in normotonic conditions. Likewise, 100 µl of cells were added to a second test tube and the volume was made up to 3 ml with double-distilled water. In this case, the sample showed 100% haemolysis and was used as positive control, as RBC lysed in a hypotonic medium. The selected nanoparticles formulation, LNP4 (1 ml), was separately added to 100 µl cell suspension. All the samples were incubated at 37°C for 1 h in a water bath. After incubation, debris and intact erythrocytes were removed by centrifugation and 100 µl of resulting supernatant was dissolved in 2 ml of ethanol/HCl mixture (39 parts of 99% ethanol and 1% HCl). This mixture dissolved all the components and prevented the precipitation hemoglobin. The absorbance of the mixture was determined at 405 nm using ELISA plate reader. The experiment was performed in triplicate. The percentage haemolysis was calculated applying the following equation (23):

$$\%\ \text{Haemolysis} = \frac{\text{absorbance of sample}}{\text{absorbance of positive control}} \times 100$$

In Vivo Toxicity Analysis

Several biochemical parameters, i.e. quantification of serum glutamic pyruvate transaminase (SGPT), serum glutamic oxaloacetic transaminase (SGOT), and alkaline phosphatase (ALP), were used as the analytical markers to assess the hepatotoxicity (16).

RESULTS AND DISCUSSION

Polymer Synthesis and Characterization

The various hydrophobic and hydrophilic polymers were synthesized by reaction of poly(dichlorophosphazene) using alkoxy, phenoxy and amine terminated substituents to yield low molecular weight polyphosphazenes according to the synthetic Scheme I. The polymers synthesized were made to be hydrophilic and hydrophobic by appropriate choice of the substituents. In our work, we used 2-propoxy and 4-formylphenoxy to impart hydrophobicity to the target polymer while hydrophilicity was attributed to the 4-acetamidophenoxy and ethyl-4aminobenzoate due to the presence of hydrolysable amide and ester bonds in respective substituents. The physicochemical and spectral data of the synthesized polymeric matrices is discussed below:

Poly[bis-(2-propoxy)]phosphazene (3)

Yield: 75.44%; IR (KBr) cm^{-1} 1395 (gem dimethyl) and 1174 (P=N str). ^{1}H-NMR (D_2O-d_6, δ ppm): 1.17–1.31 (d, 12 H, $-OCH(CH_3)_2$)and 4.70 (br, 2H, $-OCH$); ^{31}P-NMR, (DMSO-d_6, δ ppm): 1.59 s; $M_w = 1.4 \times 10^5$ daltons.

Poly[bis(4-acetamidophenoxy)]phosphazene (4)

Yield : 60.70%; IR (KBr) cm^{-1} : 3280 (N-H str), 1675 (C=O str), 1200 (P=N str) and 1160 and C-O str). ^{1}H-NMR (DMSO-d_6, δ ppm): 2.00–2.06 (s, 6H, $NHCOCH_3$), 6.64–6.68 (m, 4H, *meta*-Ar*H*), 7.30–7.34 (m, 4H, *ortho* Ar*H*), 8.97–9.55 (s, 2H, $NHCOCH_3$); ^{31}P-NMR, (D_2O-d_6, δ ppm): −10.90 s; $M_w = 1.9 \times 10^5$ daltons.

Poly[bis(4-formylphenoxy)]phosphazene (5)

Yield: 83.13%; IR (KBr): 1704 (C=O str), 1216 (P=N str), 1161 (C-O str) and 828 (aromatic bend). ^{1}H-NMR (DMSO-d_6, δ ppm): 6.91 (m, 4H, *ortho*-Ar*H*), 7.7 (m, 4H, *meta*-Ar*H*), and 9.7 (s, 2H, C*H*O). ^{31}P-NMR (DMSO-d_6, δ ppm): −7.02 s; $M_w = 1.6 \times 10^5$ daltons.

Poly[bis(4-ethoxycarbonylanilino)]phosphazene (6)

Yield: 55.76%; IR(KBr) cm^{-1}: (3434 N-H str), 1720 (C=O str), 1266 (P=N str), 1160 (C-O str) and 812 (aromatic C-H bend). ^{1}H-NMR (DMSO-d_6, δ ppm): 1.24–1.27 (t, 6H, $COOCH_2CH_3$), 4.17–4.22 (q, 4H, $COOCH_2CH_3$), 6.66–6.67 (d, 4H, *ortho*-Ar*H*), 7.62–7.64 (d, 4H, *meta*-Ar*H*), 10.26 (s, 2H, N-H); ^{31}P-NMR (DMSO-d_6, δ ppm): 1.59 s; $M_w = 2.7 \times 10^5$ daltons.

The glass transition temperatures (T_g) of the synthesized polymers are shown in Table I.

The TGA curves of these polymers are shown in Fig. 3.

Degradation Studies of Substituted Polyphosphazenes

The rate of degradation of polyphosphazenes, as in the case of water permeability to the polymer matrix, which in turn depends on the hydrophilicity / hydrophobicity of the matrix, solubility of degradation products, pH and temperature of the environment.

Table I Structural and Physical Properties of Polymers

Polymer	Formula	^{31}P-NMR (δ ppm)	T_g (°C)	M_w (Daltons)
3	$[NP(OCH(CH_3)_2]_n$	−1.59	48.19	1.4×10^5
4	$[NP(OC_6H_4NHCOCH_3)_2]_n$	−10.90	45.63	1.9×10^5
5	$[NP(OC_6H_4CHO)_2]_n$	−7.02	79.62	1.6×10^5
6	$[NP(NHC_6H_4COOC_2H_5)_2]_n$	1.59	68.19	2.7×10^5

The erosion of the poly(organophosphazenes) started with incubation in the aqueous medium. During observation crackings and the porous zones were also observed on the surface of the polymers accounting for the surface erosion mechanism of degradation of poly(organophosphazenes) as depicted in the SEM images of polymer degradation samples. Such erosion zonesare characteristic features of polymers that undergo surface erosion. The degradation products might have started transporting into the buffer media from the site of formation. Further, the poly(organophosphazenes) might have eroded either under the formation of porous erosion zones or the formation of semisolid erosion zones (e.g. polyanhydrides) (Fig. 4) (24).

The surface morphology of the degraded matrices of polymers studied by scanning electron microscopy are shown in Fig. 5, 6, and 7.

The surface morphology of the degraded matrices of polymers studied by scanning electron microscopy (SEM) are shown in Fig. 5, 6, and 7.

The polymer matrices degraded fastest at pH 5.5 (acidic media) followed by pH 6.8 and pH 7.4 except for polymer **6**. This behavior of polymer **6** might be due to the stability of

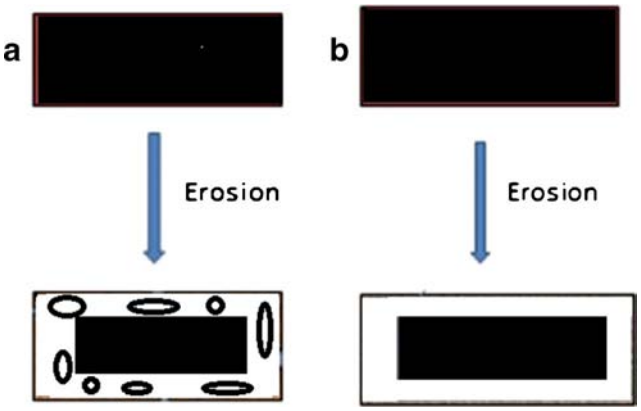

Fig. 4 Possible mechanism of erosion of poly(organophosphazenes) (**a**) erosion under the formation of porous erosion zones (**b**) erosion under the formation of semisolid erosion zones.

aromatic ester group in acidic media or the bulkier nature of the substituents.

All the substituted polymers exhibited degradation, but at different rates. For polymers **3** and **5**, the degradation was greater at pH 5.5 (74.21% and 55.95%) than at pH 6.8 and 7.4 solution (59.66% and 49.38% and 54.84% and 47.15% degradation, respectively). Polymers **4** degraded (57.34%) at pH 5.5 after 28 days, which was faster than the matrices placed in pH 6.8 and pH 7.4 solutions, that degraded 68.41% and 74.27% respectively at 35 days. Polymers **7** degraded faster at pH 7.4 (54.11% degradation) after 28 days than at pH 5.5 and 6.8 (64.95% and 70.33%, respectively) after 35 days.

The polymer matrices degraded fastest at pH 5.5 (acidic media) followed by pH 6.8 and pH 7.4 except for polymer 6. This behavior of polymer 6 might be due to the stability of

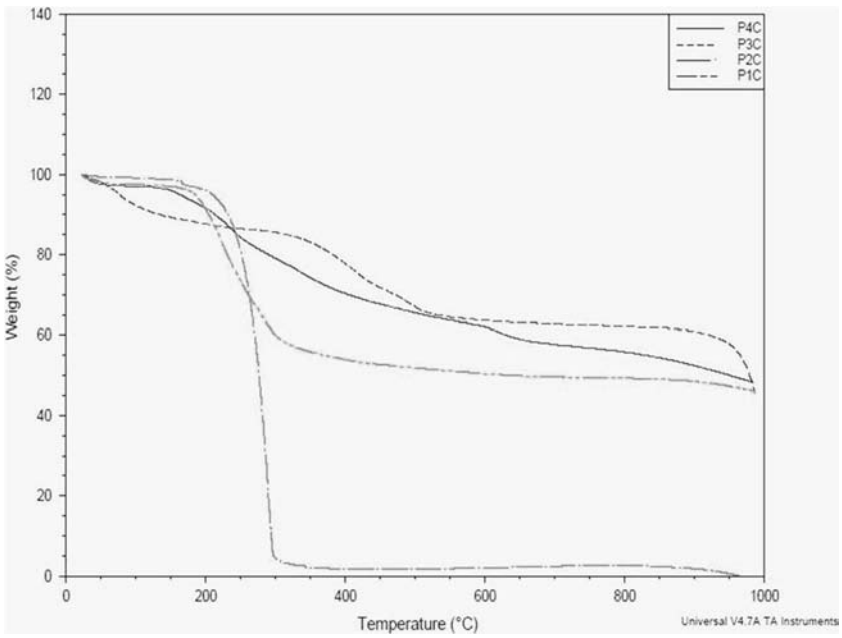

Fig. 3 TGA curves of substituted poly(organophosphazenes) (**a**) poly[bis-(2-propoxy)]phosphazene **(3)** (**b**) poly[bis(4-acetamidophenoxy)]phosphazene **(4)** (**c**) poly[bis(4-formylphenoxy)]phosphazene **(5)** (**d**) poly[bis(4-ethoxycarbonylanilino)]phosphazene **(6)**.

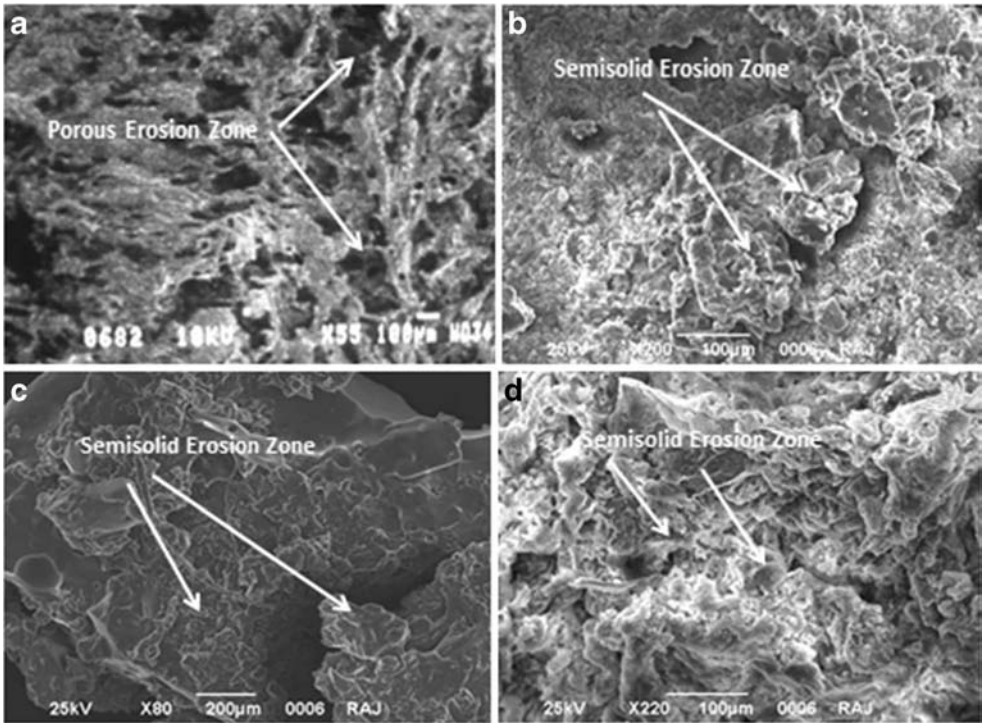

Fig. 5 Typical SEM images of eroding substituted poly(organophosphazenes) (**a**) Poly[bis-(2-propoxy)]phosphazene **(3)** (**b**) Poly[bis(4-acetamidophenoxy)]phosphazene **(4)** (**c**) Poly[bis(4-formylphenoxy)]phosphazene **(5)** (**d**) Poly[bis(4-ethoxycarbonylanilino)]phosphazene **(6)** in phosphate buffer of pH 5.5 after 35 days of incubation.

aromatic ester group in acidic media or the bulkier nature of the substituents.

All the substituted polymers exhibited degradation, but at different rates. For polymers **3** and **5** the degradation was greater at pH 5.5 (79.46 and 61.13%) than at pH 6.8 and 7.4 solution (63.27%, 52.66% and 60.68%, 48.15% degradation, respectively). Polymers **4** degraded (61.90%) at pH 5.5 after 28 days, which was faster than the matrices placed in pH 6.8 and pH 7.4 solutions, that degraded 65.51% and 69.32%, respectively at 35 days. Polymers (7)

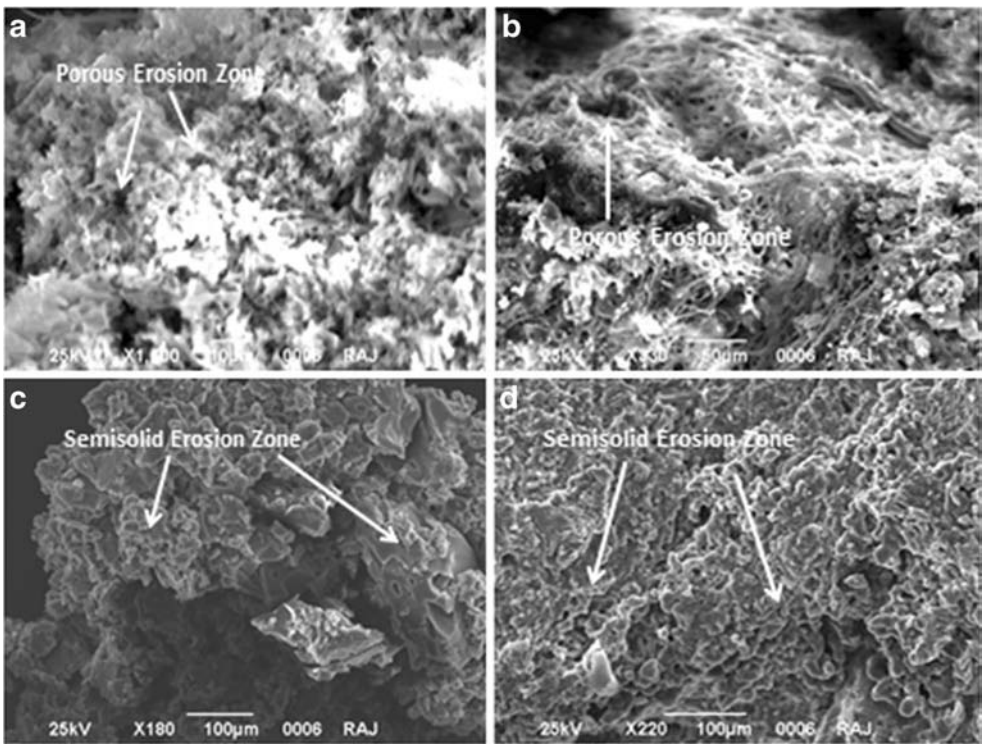

Fig. 6 Typical SEM images of eroding substituted poly(organophosphazenes) (**a**) Poly[bis-(2-propoxy)]phosphazene **(3)** (**b**) Poly[bis(4-acetamidophenoxy)]phosphazene **(4)** (**c**) Poly[bis(4-formylphenoxy)]phosphazene **(5)** (**d**) Poly[bis(4-ethoxycarbonylanilino)]phosphazene **(6)** in phosphate buffer of pH 6.8 after 35 days of incubation.

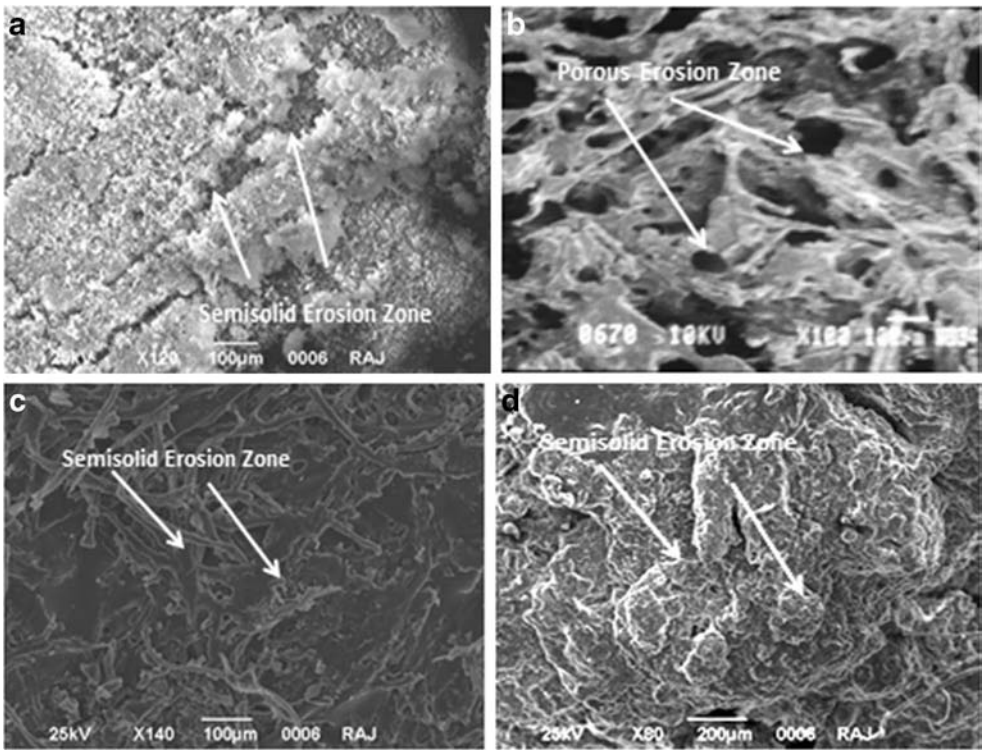

Fig. 7 Typical SEM images of eroding substituted poly(organophosphazenes) (**a**) Poly[bis-(2-propoxy)]phosphazene **(3)** (**b**) Poly[bis(4-acetamidophenoxy)]phosphazene **(4)** (**c**) Poly[bis(4-formylphenoxy)]phosphazene **(5)** (**d**) Poly[bis(4-ethoxycarbonylanilino)]phosphazene **(6)** inphosphate buffer of pH 7.4 after 35 days of incubation.

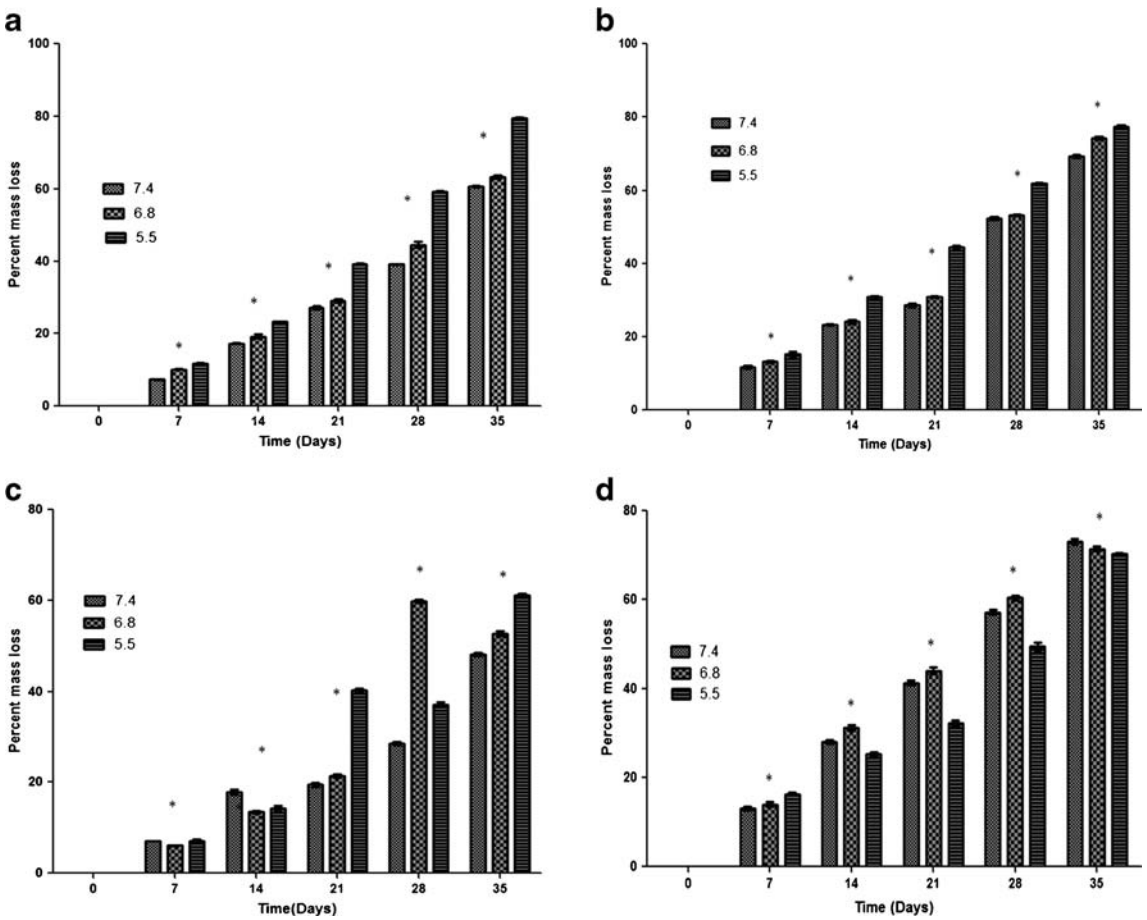

Fig. 8 Comparison of degradation pattern substituted polyphosphazenes (**a**) polymer **3** (**b**) polymer **4**, (**c**) polymer **5** (**d**) polymer **6** in different pH (pH 5.5, pH 6.8 and pH 7.4).

Table II Average Particle Size and Zeta Potential of Drug Loaded Substituted Poly(organophosphazene-s) Nanoparticles

Parameters	Formulation code			
	LNP1	LNP2	LNP3	LNP4
Percentage yield	81.8%	77.27%	79.09%	83.63%
Percentage entrapment efficiency of primaquine	31.6%	34.8%	32.5%	38.5%
Percentage entrapment efficiency of dihydroartemisinin	28.5%	31.8%	33.5%	34.9%
Percent drug loading of primaquine	5.25%	4.94%	4.77%	5.62%
Percent drug loading of dihydroartemisinin	4.28%	4.49%	4.21%	4.59%

degraded faster at pH 7.4 (57.14% degradation) after 28 days than at pH 5.5 and 6.8 (69.19% and 71.47% respectively) after 35 days.

The comparative study of all the polyphosphazenes used in the study at pH 5.5, 6.8 and 7.4. are shown in Fig. 8.

It was observed that polymer **3** and **5** degraded approximately at the same rate because of the presence of hydrophobic side groups, which resulted in decreased water permeation into matrix and a slower hydrolytic breakdown of the polymers (polymers **3** has greater degradation rate as compared to polymer **5**, because of the presence of bulkier hydrophobic benzyl group in polymers **5**). Polymer **4** followed the same pattern of degradation at all pH but at different rates. This could be because the acetamido functionality of the aromatic ring might have provided the hydrolytic unstability to the polymer, thereby, resulting in polymer breakdown.

Polymers **6** has ester functionality at the para position of the aromatic ring. This moiety might have been involved in the breakdown of polyphosphazene skeleton by hydrolysis of ester unit to form carboxylanilino, which would then have resulted in water-soluble polymers. Alternatively, the presence of water might have facilitated an attack on the polymer

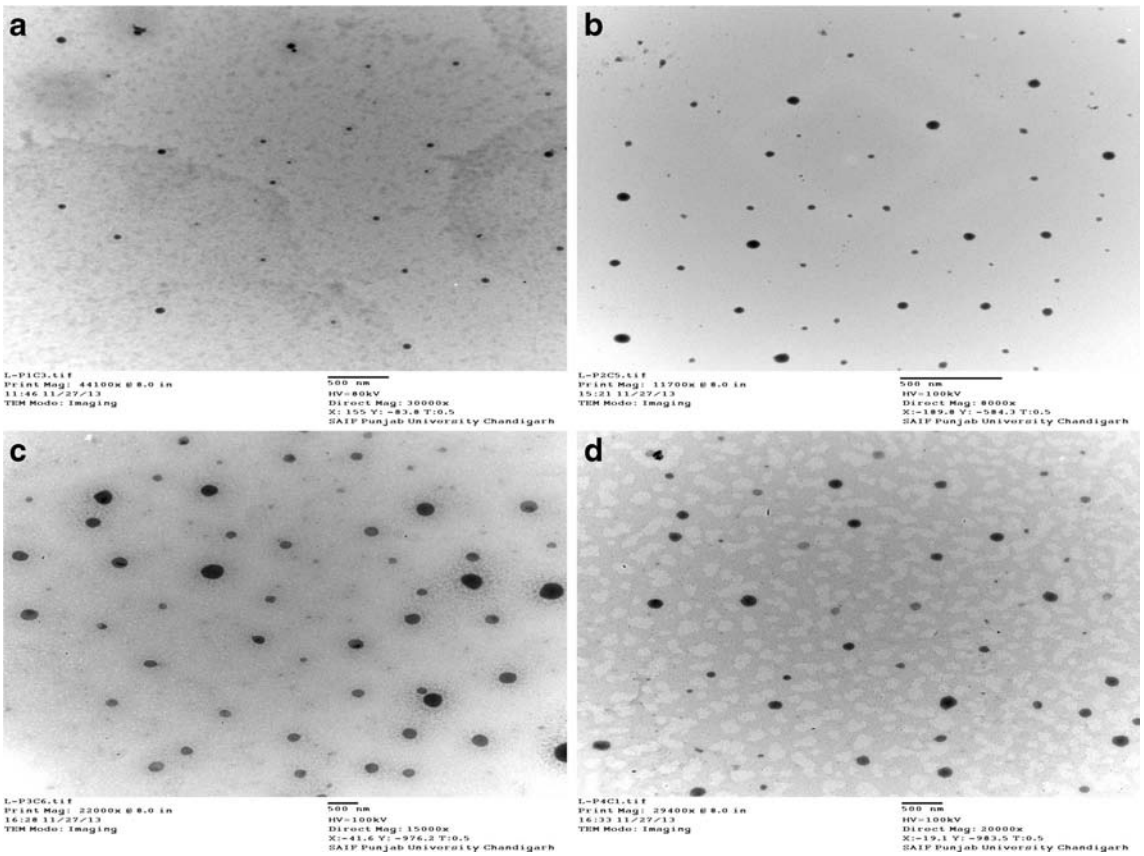

Fig. 9 TEM image of (**a**) primaquine and dihydroartemisinin Loaded poly[bis-(2-propoxy)]phosphazene nanoparticles **(LNP1)** (**b**) primaquine and dihydroartemisinin loaded poly[bis(4-acetamidophenoxy)]phosphazene Nanoparticles **(LNP2)** (**c**) primaquine and dihydroartemisinin loaded poly[bis(4-formylphenoxy)]phosphazene nanoparticles **(LNP3)** (**d**) primaquine and dihydroartemisinin loaded poly[bis(4-ethoxycarbonylanilino)]phosphazene nanoparticles **(LNP4).**

backbone by ester functionality itself. Water molecules might have then reacted with the unstable polymer-anilino bond. As a result of this reaction, the polymer bound anilino would have been released and a hydrolytic sensitive polyphosphazene could have been formed. In the third mechanism, water might have displaced the ethyl 4-carboxylanilino from the phosphorus atom to form hydroxyphosphazene. This species could have rearranged in the presence of water to a phosphazene. The phosphazene would have then reacted with water to yield phosphate and ammonia. Indeed, the polymer degradation rate is governed by several important factors as discussed for the poly(organophosphazenes) such as type of chemical bond, molecular weight, hydrophobicity, environmental conditions (pH, *in vitro*.) etc. (25). These results are supported by degradation studies of the synthesized biodegradable poly(organophosphazenes) which clearly show that the incorporation of hydrophilic, hydrophobic or bulky substituentsto the polymeric backbone can monitor the hydrolytic degradation behaviour of these polymers. The non-toxic degradation products and hydrolytic degradation behaviour of such polymers proves them to be promising delivery vehicle for the controlled release of the drug candidates (26).

Morphology, Particle Size and Zeta Potential of Nanoparticles Formulations

The average particle size of drug loaded substituted poly(organophosphazenes) nanoparticles formulation was found to be in the range of 137.4±5.7 to 240.16±2.0 nm. The Zeta potential of drug loaded substituted poly(organophosphazenes) nanoparticles formulations have been found to be ranging from −24.63±2.70 mV to −41.22 ±3.01 mV. The results of average particle size and zeta potential of different nanoparticles formulations are shown in Table II.

The TEM images for primaquine and dihydroartemisinin loaded substituted poly(organophosphazenes) nanoparticles are shown in Fig. 9.

The results of various physicochemical parameters like percent yield, entrapment efficiency and percent drug loading of drug loaded nanoparticles formulations are shown in Table III.

Table III Percent Yield, Entrapment Efficiency, Percent Drug Loading of Drug Loaded Nanoparticles Formulations

Formulation code	Average particle size	Zeta potential
LNP1	199.9±2.9	−24.63±2.70
LNP2	137.4±5.7	−35.02±2.78
LNP3	240.16±2.0	−32.09±2.77
LNP4	226.6±1.7	−41.22±3.01

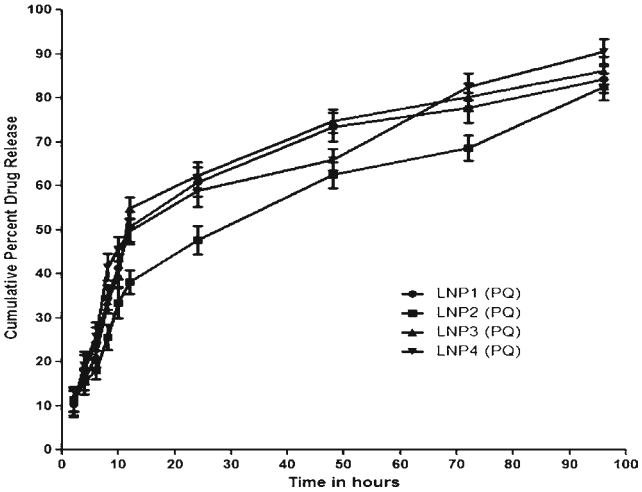

Fig. 10 *In vitro* release profile of primaquine from drug loaded substituted polyphosphazenes nanoparticles, where, primaquine and dihydroartemisinin loaded poly[bis-(2-propoxy)]phosphazene nanoparticles **(LNP1)**; primaquine and dihydroartemisinin loaded poly[bis(4-acetamidophenoxy)]phosphazene nanoparticles **(LNP2)**; primaquine and dihydroartemisinin loaded poly[bis(4-formylphenoxy)]phosphazene nanoparticles **(LNP3)**; primaquine and dihydroartemisinin loaded poly[bis(4-ethoxycarbonylanilino)]phosphazene nanoparticles **(LNP4).**

In Vitro Drug Release Studies

The release profile of primaquine and dihydroartemisinin from different nanoparticles formulations is shown in Fig. 10 and 11 respectively. It was observed that both the drugs were released from nanoparticles formulations in a biphasic pattern: initialally burst release for first 12 h followed by sustained

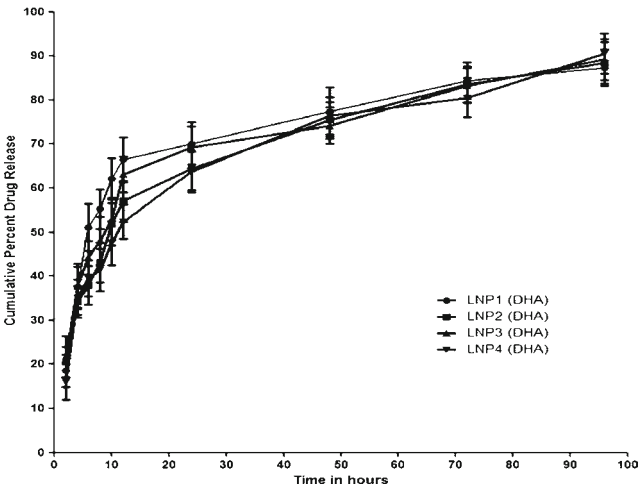

Fig. 11 *In vitro* drug release of dihydroartemisinin from drug loaded nanoparticles Formulations where, primaquine and dihydroartemisinin loaded poly[bis-(2-propoxy)]phosphazene nanoparticles **(LNP1)**; primaquine and dihydroartemisinin loaded poly[bis(4-acetamidophenoxy)]phosphazene nanoparticles **(LNP2)**; primaquine and dihydroartemisinin loaded poly[bis(4-formylphenoxy)]phosphazene nanoparticles **(LNP3)**; primaquine and dihydroartemisinin loaded poly[bis(4-ethoxycarbonylanilino)]phosphazene nanoparticles **(LNP4).**

Table IV Goodness of Fit for the Comparison of Mechanism of Release of Primaquine from Drug Loaded Nanoparticles Formulations for First Step Release (0–12 h)

Nanoparticle formulation	Zero order $Q = K_o t$		First order [ln (100-Q) = ln Q-$K_1 t$]		Higuchian $Q = Kt^{1/2}$		Korsmeyer and Peppas $Q = K_p t^n$		
	K_o	R^2	K_1	R^2	K	R^2	K_p	n	R^2
LNP1	4.01	0.996	0.05	0.983	19.53	0.972	1.69	0.88	0.993
LNP2	2.78	0.976	0.03	0.966	13.38	0.932	1.85	0.68	0.941
LNP3	4.30	0.964	0.06	0.925	20.57	0.910	1.69	0.86	0.945
LNP4	4.14	0.964	0.05	0.969	20.41	0.966	1.73	0.89	0.983

*Number of live mice/total number of mice infected.

release. The initial burst release of the drugs from nanoparticles can be explained on the basis of the fact that some portion of the drug being adsorbed onto the surface of nanoparticles formulations and the sustained release accompanied by diffusion of the drugs from the inside of the nanoparticles formulations. Further, it was observed that the nanoparticles formulations sustained the release of the drugs for 4 days. Further, in order to explore the drug release kinetics mechanism, a high degree of agreement between the coefficient of correlation was established on fitting the drug release data to different kinetic models.

In order to explore further the diffusion mechanism followed for the designed formulations, the data were plotted into Korsmeyer-Peppas equation. All the designed formulations fitted best towards Korsmeyer-Peppas model in two step release. The data for drug release kinetics from different nanoparticles formulations are shown in Tables IV, V, VI, and VII.

Where Q is the percent of the drug release at time t. K_0, K_1 and K are the coefficients of equation. Kp is constant incorporating structural and geometric characteristics of the release device and n is the release exponent indicate the release mechanism.

It was observed that different formulations showed, high exponent value of n, ($0.45 < n < 0.89$) for anomalous release, 0.89 for a case II release and > 0.89 for a super case II type drug release kinetics mechanism during first step release (0–12 h) thereby resulting in a key role of the dissolution and erosion of the polymer to the release of drug. During the first step release of primaquine, n value between 0.68 and 1.07 was observed, suggesting a release kinetics ranging from Fickian to case II transport while for dihydroartemisinin it varied from 0.54 to 0.83 thereby showing the contribution of anomalous (non-Fickian) transport from the nanoparticles formulations. During second step (12–96 h) release of both the drugs, the low exponent values close to Fickian diffusion ($n < 0.46$) were observed which is attributed to the aggregation of drugs into dialysis membrane and greater role of Fickian diffusion towards drug release. Although both the drugs showed good fitness towards the kinetics models such as zero order kinetics, first order and Higuchi yet their release mechanism is explained by their best fitness towards Korsmeyer-Peppas model. Moreover, the contributing role of bioerosion and diffusion phenomenon are responsible for drug release kinetics in biodegradable matrices such as poly(organophosphazenes). It can be concluded that during the first step release of both drugs, most of the formulations exhibited non-Fickian transport followed by Fickian diffusion during second step release. After exploring the *in vitro* evaluation of the drug loaded nanoparticles formulations, further biological evaluation for antimalarial potential was performed on the basis of formulation with highest entrapment efficiency and percent drug loading.

In Vivo Antimalarial Efficacy of Drug Loaded Nanoparticles Formulations

The *P. berghei* infected mice were treated with three doses; lower dose (0.07 + 0.07) mmol/kg, medium dose (0.11 + 0.11) mmol/kg and high dose (0.14 + 0.14) mmol/kg of the nanoparticles formulations for a period of 4 days. The results of

Table V Goodness of Fit for the Comparison of Mechanism of Release of Primaquine from Drug Loaded Nanoparticles Formulations for Second Step Release (12–96 h)

Nanoparticle Formulation	Zero Order $Q = K_o t$		First Order [ln (100-Q) = ln Q-$K_1 t$]		Higuchian $Q = Kt^{1/2}$		Korsmeyer and Peppas $Q = K_p t^n$		
	K_o	R^2	K_1	R^2	K	R^2	K_p	n	R^2
LNP1	0.37	0.931	0.01	0.983	5.18	0.979	3.33	0.24	0.993
LNP2	0.50	0.978	0.01	0.966	6.71	0.987	2.73	0.35	0.989
LNP3	0.36	0.957	0.01	0.994	4.97	0.992	3.45	0.21	0.995
LNP4	0.48	0.982	0.01	0.960	6.41	0.972	3.17	0.28	0.959

Table VI Goodness of Fit for the Comparison of Mechanism of Release of Dihydroartemisinin from Drug Loaded Nanoparticles Formulations for First Step Release (0–12 h)

Nanoparticle formulation	Zero order $Q = K_o t$		First order [ln (100-Q) = ln Q-$K_1 t$]		Higuchian $Q = Kt^{1/2}$		Korsmeyer and Peppas $Q = K_p t^n$		
	K_o	R^2	K_1	R^2	K	R^2	K_p	n	R^2
LNP1	4.53	0.912	0.08	0.969	22.97	0.967	2.54	0.70	0.955
LNP2	3.43	0.968	0.05	0.980	17.00	0.979	2.68	0.54	0.978
LNP3	3.66	0.943	0.06	0.960	18.25	0.968	2.76	0.54	0.967
LNP4	3.15	0.869	0.04	0.917	15.99	0.925	2.50	0.60	0.908

effect of drug loaded nanoparticles on parasitemia progression of *P. berghei* infected mice are summerized in Table VIII.

The values are expressed as mean ± SEM (standard error mean) significantly different from the untreated group ($p < 0.05$), $n = 6$ mice per group.

The control group (without any treatment) showed 70–80% parasitemia on day 7 and died between 8 and 15 days.

The primaquine and dihydroartemisinin nanoparticles formulations were effective in eradicating the parasites completely showing 100% antimalarial activity. This designed combination therapy and tested nanoparticles formulation provided protection over 35 days without any recrudescence at lower dose. The results of survivals of treated animals are shown in Table IX.

The photomicrographs of blood smears of treatment groups are shown in Fig. 12

It is well known that primaquine is the most suitable antimalarial drug effective at all stages of malaria, the results of our study demonstrate that addition of dihydroartemisinin could have aided to decrease parasitemia progression more effectively, providing prolonged exposure of low concentration of parasites to the immunity system. This finding is further supported by the results of earlier studies on arteether based antimalarial therapy and other such studies (27–31). All the formulations showed 100% antimalarial activity after 14 days of treatment. The results of average percent antimalarial activity and mean survival time (MST) are shown in Table X.

Table VII Goodness of Fit for the Comparison of Mechanism of Release of Dihydroartemisinin From Drug Loaded Nanoparticles Formulations for Second Step Release (12–96 h)

Nanoparticle formulation	Zero Order $Q = K_o t$		First Order [ln (100-Q) = ln Q-$K_1 t$]		Higuchian $Q = Kt^{1/2}$		Korsmeyer and peppas $Q = K_p t^n$		
	K_o	R^2	K_1	R^2	K	R^2	K_p	n	R^2
LNP1	0.25	0.979	0.01	0.993	3.45	0.997	3.83	0.13	0.973
LNP2	0.37	0.969	0.01	0.999	5.05	0.991	3.49	0.21	0.996
LNP3	0.30	0.988	0.01	0.976	4.03	0.982	3.72	0.16	0.960
LNP4	0.42	0.947	0.01	0.967	5.72	0.981	3.33	0.25	0.990

Table VIII Effect of Drug Loaded Nanoparticles on Parasitemia Progression of *P. berghei* Infected Mice. For Each Group $n = 6$

Treatment Groups	Dose (mmol/kg)	Percent Parasitaemia (mean ± S.D.)					
		4 days	7 days	14 days	21 days	28 days	35 days
Control	–	29.91 ± 3.52	76.11 ± 7.09	–	–	–	–
PQ & DHA	(0.07 + 0.07)	3.03 ± 0.68	2.85 ± 0.65	0.0 ± 0.0	0.0 ± 0.0	0.0 ± 0.0	0.0 ± 0.0
PQ & DHA	(0.11 + 0.11)	2.05 ± 0.32	1.78 ± 0.46	0.0 ± 0.0	0.0 ± 0.0	0.0 ± 0.0	0.0 ± 0.0
PQ & DHA	(0.14 + 0.14)	1.56 ± 0.25	1.11 ± 0.40	0.0 ± 0.0	0.0 ± 0.0	0.0 ± 0.0	0.0 ± 0.0
LNP4	(0.07 + 0.07)	3.45 ± 0.52	2.8 ± 0.44	0.0 ± 0.0	0.0 ± 0.0	0.0 ± 0.0	0.0 ± 0.0
LNP4	(0.11 + 0.11)	3.25 ± 0.43	2.68 ± 0.51	0.0 ± 0.0	0.0 ± 0.0	0.0 ± 0.0	–
LNP4	(0.14 + 0.14)	2.76 ± 0.46	2.56 ± 0.36	0.0 ± 0.0	0.0 ± 0.0	0.0 ± 0.0	–

Table IX Effect of Drug Loaded Nanoparticles Formulations on Survival of *P. berghei* Infected Mice

Treatment Groups	Dose (mmol/kg)	Number of survivals*					
		4 days	7 days	14 days	21 days	28 days	35 days
Control		6/6	6/6	1/6	0/6	0/6	0/6
PQ & DHA	(0.07 + 0.07)	6/6	6/6	6/6	6/6	6/6	6/6
PQ & DHA	(0.11 + 0.11)	6/6	6/6	6/6	6/6	6/6	5/6
PQ & DHA	(0.14 + 0.14)	6/6	6/6	6/6	6/6	5/6	4/6
LNP4	(0.07 + 0.07)	6/6	6/6	6/6	6/6	6/6	4/6
LNP4	(0.11 + 0.11)	6/6	6/6	6/6	6/6	5/6	0/6
LNP4	(0.14 + 0.14)	6/6	6/6	6/6	5/6	4/6	0/6

*Number of live mice/total number of mice infected.

The infected mice treated with lower dose of (0.07 + 0.07) mmol/kg showed decrease in parasitemia progression most effectively and prolonged the life span.

In Vitro Erthrocytic Toxicity Assay

The haemolytic study was carried out to evaluate the cytotoxicity of the formulation. Haemolysis is considered an important parameter and needs to be tested when the formulations are designed to act on blood stage. Positive control (double-distilled water) showed 100% haemolysis of RBC. The percentage of haemolysis observed in the tested formulations, i.e. Standard and LNP4 was 3.7% and 4.3% respectively. The percentage of haemolysis induced by nanoparticles formulations remained within the acceptable range for i.v. administration.

In Vivo Toxicity Analysis

The obtained values for the various biochemical parameters such as serum glutamic pyruvate transaminase (SGPT), serum glutamic oxaloacetic transaminase (SGOT), and alkaline phosphatase (ALP) are depicted in Table XI.

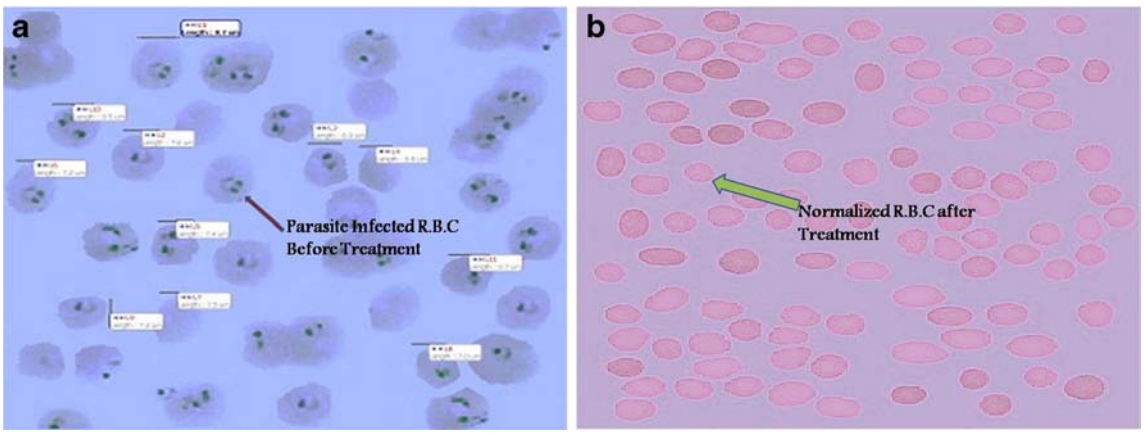

Fig. 12 Photomicrographs of blood smears of treatment groups (**a**) parasite infected RBCs before treatment (**b**) normalized RBCs after treatment with drug-loaded nanoparticles formulations.

Table X The Percent Average Activity and Mean Survival Time of Tested Drug Loaded Nanoparticles Formulation Against *Plasmodium berghei* Infected Mice

Treatment groups	Dose (mmol/kg)	% Average activity on day 4 of treatment	%Average Activity on day 7 of treatment	% Average activity on day 14 of treatment	Mean survival time (days) (MST)
Control	–	–	–	–	12.16 ± 4.11
PQ & DHA	(0.07 + 0.07)	89.86	96.25	100	>35
PQ & DHA	(0.11 + 0.11)	93.14	97.65	100	34.16 ± 2.04
PQ & DHA	(0.14 + 0.14)	94.76	98.53	100	33 ± 3.63
LNP4	(0.07 + 0.07)	88.46	96.32	100	33.66 ± 2.16
LNP4	(0.11 + 0.11)	89.13	96.47	100	30 ± 2.82
LNP4	(0.14 + 0.14)	90.75	96.62	100	28.33 ± 4.96

Table XI Serum Biochemistry Parameters Evaluated After *In Vivo* Toxicity Studies

S. No.	Formulation code	SGPT (IU/L)	SGOT (IU/L)	ALP (IU/L)
1.	Control	38.70 ± 3.18	26.09 ± 3.92	123.16 ± 4.16
2.	Standard	32.30 ± 4.07	30.26 ± 4.43	129.28 ± 10.32
3.	LNP4	32.27 ± 2.83	33.27 ± 3.46	133.26 ± 24.18

The results were in the acceptable range of safety profile of the developed nanoparticles formulations.

CONCLUSION

The novel poly(organophosphazenes) bearing hydrophilic and hydrophobic side groups have been synthesized and their thermal and hydrolytic properties were evaluated. The substituted polyphosphazenes have been successfully employed as matrices materials for novel drug delivery applications. Moreover, the inherent hydrolytic biodegradability of poly(organophosphazenes), make them an extremely potential candidates of materials for novel drug delivery systems with a distinctive combination of physicochemical properties. The synthesized poly(organophosphazenes) bearing different functional moieties account for effective drugs release and targeting the drugs to the desired sites of action. Further, the design and formulation of nanoparticles of such polymeric matrices enhance the uptake of drugs by infected cells, thereby providing an efficient nanocarrier drug delivery system. The biological evaluation of the tested nanoparticles formulation showed that lower dose of (0.07 + 0.07) mmol/kg nanoparticles formulations cured the animals with complete eradication of the parasite and prolonged the survival of animals indicating that combination is effective at low dose which can be remarked as the curative dose. However, the nanoparticles formulation showed 100% antimalarial activity at all the doses. Further, the antimalarial activity of tested nanoparticles formulation was comparable with the standard drug combination clearing more parasites from blood on day 7 at lower dose of (0.07 + 0.07) mmol/kg. These results are attributed to a burst release followed by a sustained release of the drugs from the developed nanocarrier systems. Thus, this novel combined drug regimen is an alternative treatment strategy for the drug-resistant malaria.

ACKNOWLEDGMENTS AND DISCLOSURES

The authors acknowledge the financial support received from Life Science Research Board (LSRB) of Defense Research and Development Organization (DRDO), New Delhi (India) DL/81/48222/LSRB-232/SH & DD/2011. We are also thankful to Sh. Parveen Garg, Chairman, I.S.F. College of Pharmacy, Moga (Punjab) (India) for providing the necessary facilities to carry out the research work. We also acknowledge Punjab Technical University, Jalandhar (Punjab) (India) for providing necessary facilities for research work.

REFERENCES

1. Allcock HR. Inorganic polymers. New York: Allyn and Bacon; 1995.
2. Potin PH, Jeager RD. Polyphosphazenes: synthesis, structure, properties, application. Eur Polym J. 1991;4(5):341–58.
3. Allcock HR. Chemistry and applications of polyphosphazenes. Wiley: Hoboken; 2003.
4. Allcock HR. Recent developments in polyphosphazene materials science. Curr Op Solid St. 2006;10:231–40.
5. Luten J, Steenbergen VMJ, Lok MC, Graaff DAM, Nostrum VCF, Talsma H, *et al.* Degradable PEG-folate coated poly(DMAEA-co-BA)phosphazene-based polyplexes exhibit receptor-specific gene expression. Eur J Pharm Sci. 2008;33:241–51.
6. Allcock HR, Steely LB, Singh A. Hydrophobic and superhydrophobic surfaces from polyphosphazenes. Polym Int. 2006;55:621–5.
7. Sethuraman S, Nair LS, El-Amin S, Nguyen MT, Singh A, Krogman N, *et al.* Mechanical properties and osteocompatibility of novel biodegradable alanine based polyphosphazenes: Side group effects. Acta Biomater. 2010;6:1931–7.
8. Ottenbrite RA, Albertsson AC, Scott G, Vert M, Feijen J, Albertsson A, Scott G, Chiellini E. Biodegradable Polymers and Plastics. 1992;73–92.
9. Siepmanna J, Gpferichb A. Mathematical modeling of bioerodible, polymeric drug delivery system. Adv Drug Deliv Rev. 2001;48:229.
10. Laurencin CT, Morris CD, Jacques HP, Schwartz ER, Keaton AR, Zou L. Osteoblast culture on bioerodible polymers: studies of initial cell adhesion and spread. Polym Adv Tech. 1992;3:359–64.
11. Lee SM, Chun CJ, Heo JY, Song SC. Injectable and thermosensitive poly(organophosphazene) hydrogels for a 5-fluorouracil delivery. J Appl Polym Sci. 2009;113:3831–9.
12. Kang GD, Heo JY, Jung SB, Song SC. Controlling the thermosensitive gelation properties of poly(organophosphazenes) by blending. Macromol Rapid Commun. 2005;26:1615–8.
13. Sharma R, Rawal RK, Malhotra M, Sharma AK, Bhardwaj TR. Design, synthesis and ex-vivo release studies of colon-specific polyphosphazene–anticancer drug conjugates. Bioorg Med Chem. 2014;22:1104–14.
14. Singla N, Sharma R, Bhardwaj TR. Design, synthesis and *in-vitro* evaluation of polymer-linked prodrug of methotrexate for the targeted delivery to the colon. Lett Drug Des Discov. 2014;11:601–10.
15. Murthy RSR, Sapariya B, Solanki A. Sustained release implants of chloroquine phosphate for posible use in chemoprophylaxix of malaria. Indian J Exp Biol. 2001;39:902–5.
16. Aditya NP, Patankar S, Madhusudhan B, Murthy RSR, Souto EB. Arthemeter-loaded lipid nanoparticles produced by modified thin-film hydration: Pharmacokinetics, toxicological and in vivo antimalarial activity. Eur J Pharm Sci. 2010;40:448–55.
17. Kumar S, Singh RK, Sharma R, Murthy RSR, Bhardwaj TR. Design, synthesis and evaluation of antimalarial potential of polyphosphazene linked combination therapy of primaquine and dihydroartemisinin. Eur J Pharm Sci. 2014. doi:10.1016/j.ejps.2014.09.023.
18. Sohn YS, Cho YH, Baek H, Jung OS. Synthesis and properties of low molecular weight polyphosphazenes. Macromolecules. 1995;28:7566–8.

19. Gumusderelioglu M, Gur A. Synthesis, characterization: *in vitro* degradation and cytotoxicity of poly[bis(ethyl-4-aminobutyro)phosphazene]. React Funct Polym. 2002;52:71–80.
20. Huang KJ, Zhu CH. The production and characteristics of solid lipid nanoparticles. Biomaterials. 2003;24:1781–5.
21. Peters W, Robinson BL. The chemotherapy of rodent malarial. Studies on puronaridine and other manich base antimalarials. Ann Trop Med Parasitol. 1992;86:455–65.
22. Mengiste B, Makonnen E, Urga K. *In vivo* antimalarial activity of *Dodonaea angustifolia* seed extracts against *Plasmodium berghei* in mice model. MEJS. 2012;4:47–63.
23. Raina N, Goyal AK, Pillai CR, Rath G. Development and characterization of artemether loaded solid lipid nanoparticles. IJPER. 2013;47(2):123–8.
24. Burkersroda FV, Schedl L, Gopfericha A. Why degradable polymers undergo surface erosion or bulk erosion? Biomaterials. 2002;23:4221–31.
25. Deng M, Nair LS, Nukavarapu SP, Kumbar SG, Jiang T, Weikel AL, *et al*. Porous structures: *in situ* porous structures: a unique polymer erosion mechanism in biodegradable dipeptide-based polyphosphazene and polyester blends producing matrices for regenerative engineering. Adv Funct Mater. 2010;20:2743.
26. Lakshmi S, Katti DS, Laurencin CT. Biodegradable polyphosphazenes for drug delivery applications. Adv Drug Deliv Rev. 2003;55:467–82.
27. Reddy RC, Vathsala PG, Keshamouni VG. Curcumin for malaria therapy. Biochem Biophys Res Commun. 2005;326:472–4.
28. Matthew C, Amy C, Robyn TB. Inhibition of intestinal tumors by curcumin is associated with changes in the intestinal immune cell profile. J Surg Res. 2000;89:169–75.
29. Golenser J, Domb A, Teomim D. The treatment of animal models of malaria with iron chelators by the use of a novel polymeric device for slow drug release. J Pharmacol Exp Ther. 1997;281:1127–35.
30. Crommelin DJA, Eling WMC, Steerenberg PA. Liposome and immunoliposome for control release or site specific delivery of antiparasitic drugs and cytostatics. J Control Release. 1991;161:47–154.
31. Aditya NP, Chimote G, Gunalan K, Banerjee R, Patankar S, Madhusudhan B. Curcuminoids-loaded liposomes in combination with arteether protects against *Plasmodium berghei* infection in mice. Exp Parasitol. 2012;131:292–9. doi:10.1016/j.exppara.2012.04.010.